

# Use of normalized porosity in models for the porosity dependence of mechanical properties

R. W. RICE

*E-mail: roywrice@aol.com*

The use of normalized porosity in models for the porosity dependence of mechanical properties is addressed first for the frequently used power law expression for such dependence, i.e.,  $E/E_0 = (1 - P)^n$  where  $E$  is the property of interest at any volume fraction porosity ( $P$ ) and  $E_0$  is the value of  $E$  at  $P = 0$ . Normalizing  $P$  by  $P_C$ , the value of  $P$  at which the property of interest inherently goes to zero, giving  $E/E_0 = (1 - P/P_C)^n$ , clearly calls attention to the importance of  $P_C$  values  $< 1$  (e.g., potentially as low as  $\sim 0.2$ ), a fact long known but inadequately recognized. Serious problems from the arbitrary use of both  $n$  and  $P_C$  as fitting parameters with little or no guidance as to the dependence that  $n$  and  $P_C$  (which is microstructurally sensitive) have on the type of porosity are shown. Further, porosity normalization of the power law model indicates at best limited compression of different porosity dependences into a single universal porosity dependence function and little distinguishing of property dependences as a function of the type of porosity. However, normalized porosity of minimum solid area (MSA) models gives a single universal porosity dependence. The difference in responses to  $P$  normalization of the two modeling approaches is attributed to their being based respectfully on little or no pore character and on detailed pore character. Thus,  $P$  normalization may be a valuable tool for evaluating porosity models, but must be applied in a more rigorous fashion, i.e.,  $P_C$  determined primarily by measurement and correlation with the type of porosity (as with MSA models) and not as an arbitrary fitting parameter as used in the evaluations of the power law model.

© 2005 Springer Science + Business Media, Inc.

## 1. Introduction

A frequently used power law expression for the dependence of some, especially mechanical, properties on volume fraction porosity ( $P$ ) based on some modeling and empirical results has the form  $(1 - P)^n$  for the ratio of the property at any  $P$  to that at  $P = 0$ , e.g., for the ratio of Young's modulus ( $E$ ) at some  $P$  to that at  $P = 0$ ,  $E_0$ , i.e.,  $E/E_0 = (1 - P)^n$ . It has long been known, but not necessarily widely recognized, that while some types of porosity in bodies inherently can extend to  $P$  values of nearly 1 (the ultimate limit), many types of porosity cannot exist in solid bodies above lower values of  $P$ . Thus, some types of porosity, especially those left from incomplete consolidation of powders, cannot extend to higher values of  $P$ , reflective of modest green densities in such bodies. These limiting values of  $P$ , designated  $P_C$ , above which solid behavior does not exist, commonly range from  $\sim 0.25$ – $0.5$  to very nearly 1 depending on pore character. Greater recognition of the range of  $P_C$  values led to the empirical suggestion that  $P$  in the above expression for the porosity dependence of some properties can be replaced by the normalized porosity, i.e., by the ratio  $P/P_C$ , so the porosity dependence becomes  $(1 - P/P_C)^n$ . Though such  $P$  normalization has been previously suggested by some modeling, e.g., of Bert [1, 2], it has more recently been suggested and evaluated on an empirical basis [3–5].

The suggested  $P$  normalization is intuitively appealing and has now been used by several investigators, but generally without critical evaluation of specifics of the use of such a normalized expression and there has apparently been no evaluation of such normalization of  $P$  applied to other models for the porosity dependence of properties.

This paper provides an evaluation of the applicability of the above porosity normalization for elastic moduli, particularly Young's modulus, of ceramics, i.e., of the form:  $E/E_0 = (1 - P/P_C)^n$ , by first summarizing usage of this equation. Then its use is evaluated for some types of important model porosities and then for some actual porous bodies whose pore character in part or substantially approaches some of the important types of model porosity. Subsequently, application of such  $P$  normalization to another important set of models of the porosity dependence of mechanical properties based on minimum solid area (MSA) concepts is considered indicating very promising results.

Consider Literature Determinations of  $n$  and  $P_C$  values for the normalized model of the form  $(1 - P/P_C)^n$ . Phani [3] used the form  $(1 - P/P_C)^n$  for empirically fitting elastic properties as a function of  $P$  using both  $n$  and  $P_C$  values as fitting parameters first for 3 similar ThO<sub>2</sub> bodies. He obtained  $n$  values of 1.1–1.5 for both Young's ( $E$ ) and shear modulus ( $G$ ), with 5 of 6  $P_C$

values being respectively 0.38–0.39 and 0.55–0.58. No rationale was given for the ~50% difference of  $P_C$  value of 0.92 for 1 body (which showed some deviations in the porosity dependence from the other 2 bodies for  $G$ ). Phani and Niyogi [4] then fitted Young's modulus data for 4 sintered alumina bodies giving  $n$  values of 1.37–4.1 and  $P_C$  values of 0.46–1. Subsequently they [5] fitted Young's modulus data for 7 sintered rare earth oxides giving  $n$  values of 0.7–1.3 and  $P_C$  values of 0.37–0.53.

Several authors have since used the above normalized  $P$  dependence following Phani. Thus, Lam *et al.* [6], referring to Phani and Niyogi's [5] above fitting of Young's modulus data for 7 sintered rare earth oxides giving  $n$  values of 0.7–1.3 (and  $P_C$  values of 0.37–0.53), used an  $n$  value of 1, i.e., a linear relation for fitting their data, neglecting the fact that the observed range of differences in  $n$  values can mean over an order of magnitude difference in property values at higher  $P$  levels. Their two pressed and sintered alumina bodies gave  $P_C$  values of 0.5 and 0.62 (from measured green densities) for not only  $E$ , but also for fracture toughness ( $K$ ) and flexural strength. Rödel and colleagues [7, 8] reported fitting their Young's modulus (and  $K$ ) data to Phani's expression in two studies. One study of pressed and sintered alumina [5] gave  $n = 1.15$  and  $P_C = 0.4$  and the other of both a pressed and sintered as well as hot pressed alumina gave  $n = 1.35$  and  $P_C \sim 0.5$  for both  $E$  and  $K$  [8]. Roberts and Garboczi [9] reported that using  $n = 2.23$  and a  $P_C$  value of 0.65 worked well as empirical parameters in fitting Young's modulus data for  $P \leq 0.5$ . They did not discuss the variation of  $P_C$  with pore character, which is surprising since Garboczi *et al.* [10, 11] discussed some of these effects for tubular pores. More recently Kováčik [12] has reported  $n$  and  $P_C$  being nominally the same for  $E$  and  $G$  for each of 3 sets of  $\text{ThO}_2$  data (the same sets evaluated by Phani [3]), and one set each for  $\text{ZnO}$ ,  $\text{Fe}$ , and  $\text{TiAl}$  (all sintered materials) with  $P_C$  values 0.37 to 0.54 giving  $n$  values of 1.0 to 1.2.

Three critical issues need to be addressed. The first and easiest issue is the legitimacy of obtaining values of  $n$  and  $P_C$  using both as fitting parameters rather than using models, data, or both to determine  $P_C$  values. Thus, Phani and colleagues [3–5] apparently made little or no use of literature sources such as minimum solid area (MSA) models [2, 13, 14] that independently indicate some theoretical  $P_C$  values as well as some empirical values from substantial data. For the materials they considered  $P_C$  values are most likely in the range of 0.35–0.6, and these should be nearly, if not, identical for Shear ( $G$ ) and Young's ( $E$ ) moduli. Kováčik [12] has addressed this issue showing that percolation theories also show the same or very similar  $P_C$  values are obtained for  $E$  and  $G$ . There are also issues of using  $P/P_C$  instead of  $P$  alone in  $1 - P$ , i.e.,  $n = 1$ , which is the theoretical upper limit to the porosity dependence of properties considered here [2]. Thus, while there may be some utility to strictly empirical fitting of the equation to data, this can give some very misleading results and is of limited value in gaining understanding of the porosity dependence of properties.

The second and third issues are related and more complex. They are the correlation of  $P_C$ ,  $n$ , or both values with the type of porosity and with each other as a function of the amount and type of porosity. This includes the applicability of the model over a range of types and levels of porosity, especially high levels of  $P$ , e.g., approaching  $P_C$  values. Thus, in the above survey of the limited literature, most  $n$  values are between ~1.0 and ~1.5 (much of which probably reflects most bodies studied being made by consolidation of powders), but there are higher  $n$  values, e.g., from 2 to 4+. The latter may well reflect effects of empirical fitting of data, but may also reflect some differences in the nature of the porosity, which has been severely neglected. (Note that Bert [1, 2] proposed that  $n = \alpha P_C$ , where  $\alpha$  = the maximum pore stress concentration, but validity of this is uncertain due to the mixed and limited effects of stress concentrations [2].)

Broader comparison of  $P_C$  and  $n$  values for Young's and shear modulus for the same bodies indeed shows that good fits of the porosity dependence of these two properties can be obtained with nearly, or identical, values of  $P_C$ . However, exploring the interrelation of  $P$  and  $n$  by plotting  $n$  versus  $P_C$  for  $E$  (for which there is most data) in Fig. 1 reinforces and extends the above observations and questions about  $n$  and  $P_C$  values. First note that most of the data falls in the  $P_C$  range of 0.37 to 0.52, which is reasonable since all bodies evaluated were derived by sintering of powder compacts which typically cover such a range. Second, note three alumina values [4] plotted at the extreme of allowed  $P_C$  value of ~1 [2] determined by using both  $n$  and  $P_C$  as fitting variables. These three values are well outside of the range of most of the other alumina or other material data, and that these three alumina values and all other data points (except one for aligned tubular pores discussed below) suggest that  $n$  values rise, some significantly, as  $P_C$  values increase. This correlation of  $n$  values increasing with increased  $P_C$  values is also supported by the computer modeling results of Roberts and Garboczi [9]. However, the level of  $P_C$  values that are respectively impossible or unlikely to occur in bodies with pores derived from incomplete sintering of compacted particles must be questioned. Thus, while higher  $P_C$  and  $n$  values occur from using both as fitting parameters, they are not necessarily physically meaningful. In fact, note that while  $P_C$  values  $\geq 1$  are allowed mathematically they have no physical meaning. Third, note the point plotted in Fig. 1 for both model and measured data for bodies with tubular pores aligned parallel to the stress axis, which is also the upper limit of properties for porous bodies, is clearly in marked contrast in  $n$  values in comparison to the three alumina bodies fitted with  $P_C \sim 1$ . This suggests either that the extreme alumina points are incorrect, or that there are significantly different trends for different types of pores (which have not previously been observed since the effect of pore type on such property behavior has been totally neglected), or some combination of these. Fourth, note that the rest of the ceramic data agrees with data for the two metallic materials (sintered iron and a titanium aluminide [12]), which is consistent with similar porosity dependences

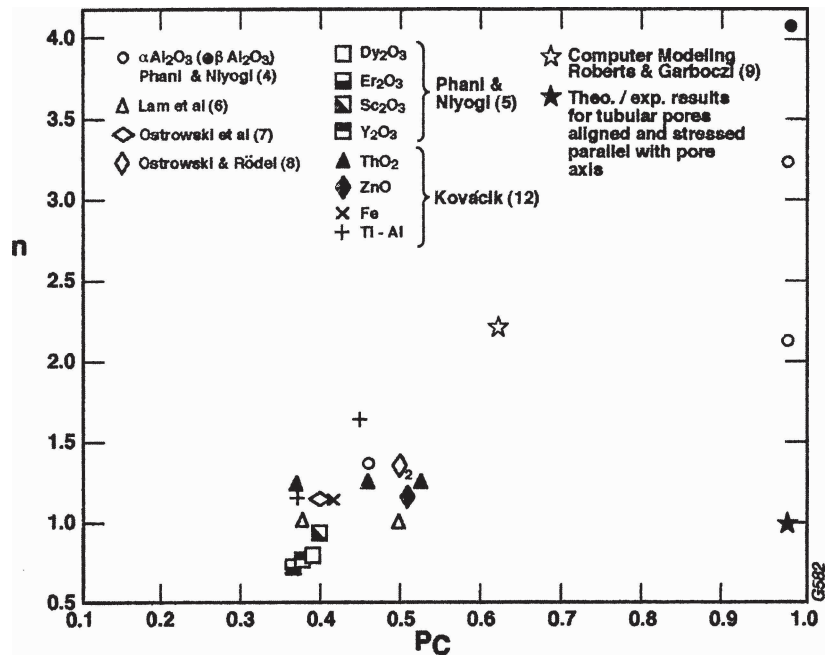


Figure 1 Plot of  $n$  versus  $P_C$  values from studies of fitting data to the power law model for the porosity dependence of Young's modulus for various sintered ceramics and two sintered metallic materials are shown. A data point from a computer modeling study [9], and a point for both experimental and theoretical data for materials with tubular pores aligned parallel with the stress axis [2] are also shown. The number 2 next to an alumina body reflects two coincident data points.

found for porous metals and porous ceramics [2], i.e., the ratio  $E/E_0$  removes the material dependence leaving the porosity dependence.

## 2. Plotting power law models of elastic properties using normalized porosity

Other issues of porosity normalization, i.e., of replacing  $P$  by  $P/P_C$ , remain, namely effects of porosity type, that are now addressed by focusing on plotting data for specific types of porosity [2, 13, 14–24].

Consider first linear plots of the relative elastic moduli versus  $1 - P/P_C$ , i.e., with  $n = 1$  in Fig. 2), e.g., with  $n$  in the normalized power law relation being nearly or exactly 1, e.g., as respectively suggested by Lam *et al.* [6] and shown by various models for cylindrical pores aligned parallel with the stress [2]. Fig. 2A shows such behavior for MSA models and the substantial data they represent [2] for tubular pores (aligned parallel or perpendicular to the applied stress) and spherical or cubic pores. These have amongst the highest  $P_C$  values ( $\sim 0.8$  to  $\sim 1$ ) and thus make limited to almost no change in normalized values of  $P$ , providing a valuable reference. Fig. 2B is a linear plot of MSA models for simple cubic (i.e.,  $\sim$  random) and a denser packing of uniform spherical particles, data for two glass bodies made by sintering nominally randomly packed glass beads, and for a pressed and sintered alumina body reflecting lower  $P_C$  values, e.g., 0.25–0.5. Fig. 2C is a linear plot of data for slip cast and foamed  $\text{SiO}_2$ , and pressed and extruded graphite and ceramic superconductor with the slip cast and pressed bodies reflecting lower  $P_C$  values and extruded bodies higher  $P_C$  values due to much of the porosity in extruded bodies commonly being approximately tubular pores.

To be valid over the full  $P$  range all Fig. 2 plots must go through the two diagonal end points of 0.0

and 1.1. Thus, while these figures all have significant sections that are approximately linear, most must be bilinear, trilinear, or nonlinear to cover the full range of porosity. More generally note that: [1] While there is some grouping of normalized plots, there can still be some significant differences in plots of different bodies with the same or similar types of porosity (e.g., for bodies of sintered glass beads, Fig. 2C), and [2]. There is no clear pattern of what types of pores give what type of plots in what location other than for tubular pores aligned with the stress axis versus other pores.

Going to semi log plots using normalized porosity values, i.e., either as  $1 - P/P_C$  or  $P/P_C$ , results in more commingling of curves and less curve sections that are approximately linear for various models or data set, e.g., Fig. 3, making distinction between them difficult with even modest experimental scatter. As previously reported log-log plots also have similar or more severe problems of distinction of different porosity types and resultant behavior [2].

## 3. Use of porosity normalization with MSA models of the porosity dependence of properties

Normalization of porosity for mechanical property evaluation as discussed earlier is not restricted to any one model, though it has thus far been used with only the power law model considered above. (It is also not necessarily limited to mechanical or conductive properties, but is clearly attractive for them given the existence of distinct  $P_C$  values for different pore structures.) Application of porosity normalization to MSA models [2, 13, 14] was considered, with particularly interesting results. Plotting values for the same key MSA models as used in the previous section, specifically those for

rhombohedral or simple cubic packing of sintering uniform spherical particles, for tubular pores aligned normal or parallel to the stress axis, and for uniform spherical pores as a function of  $P/P_C$  instead of  $P$  alone. Plotting versus  $P/P_C$  resulted in a nominally single curve located in the limited spacing between the plots for cylindrical pores aligned parallel with the stress axis (the upper limit) and for spherical pores in simple cubic packing (Fig. 4).

This initial evaluation shows far more consolidation of individual MSA curves for each of the idealized pore structures when they are plotted versus  $P/P_C$  instead of  $P$  alone in contrast to the very limited effect in normalization of the power law model, e.g., contrast Figs 2 and 4. Thus, there is very limited effect of normalization for tubular pores aligned with the stress axis (being the upper limit of property values for porous bodies) and somewhat more for spherical pores, then more

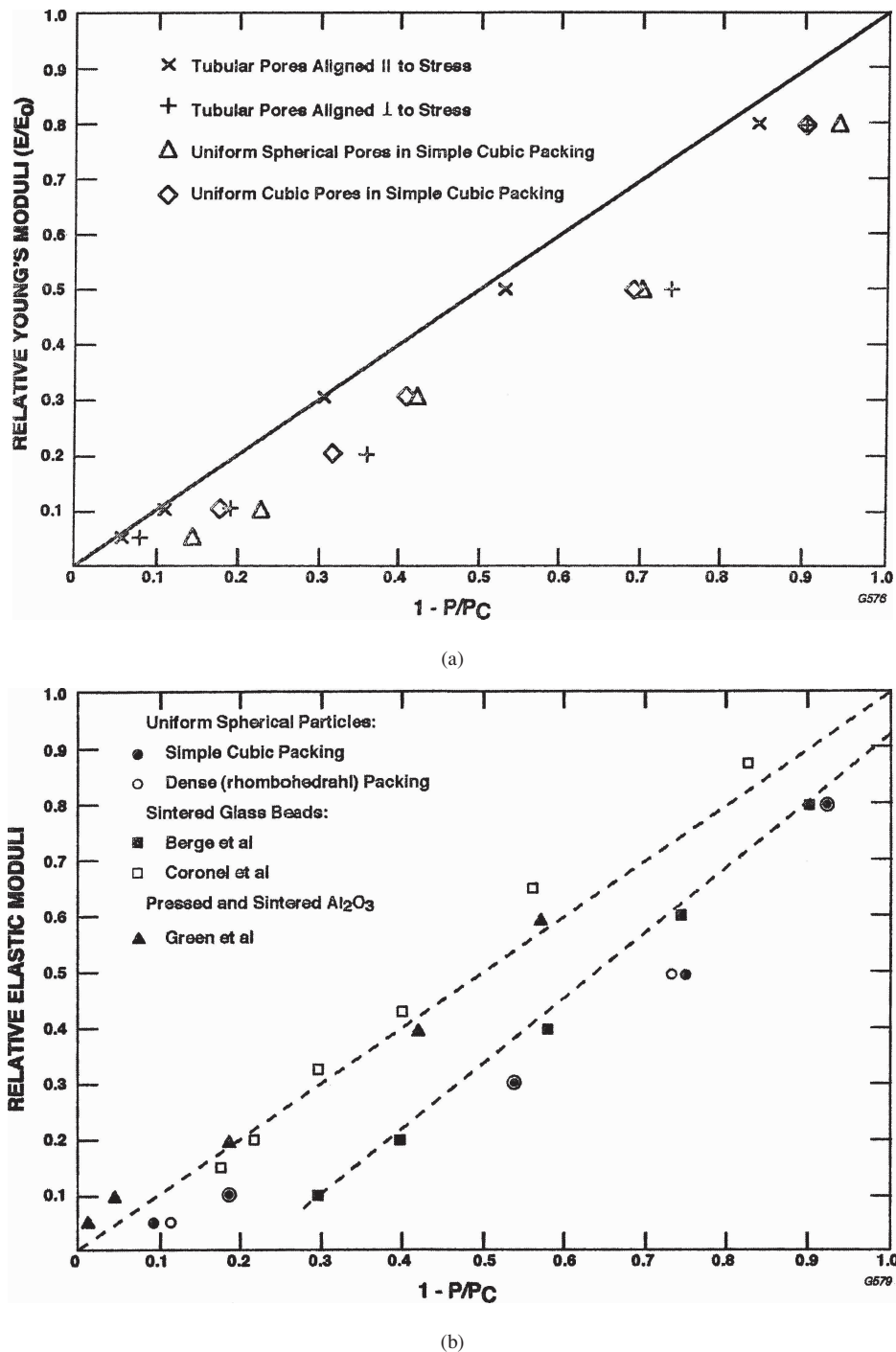
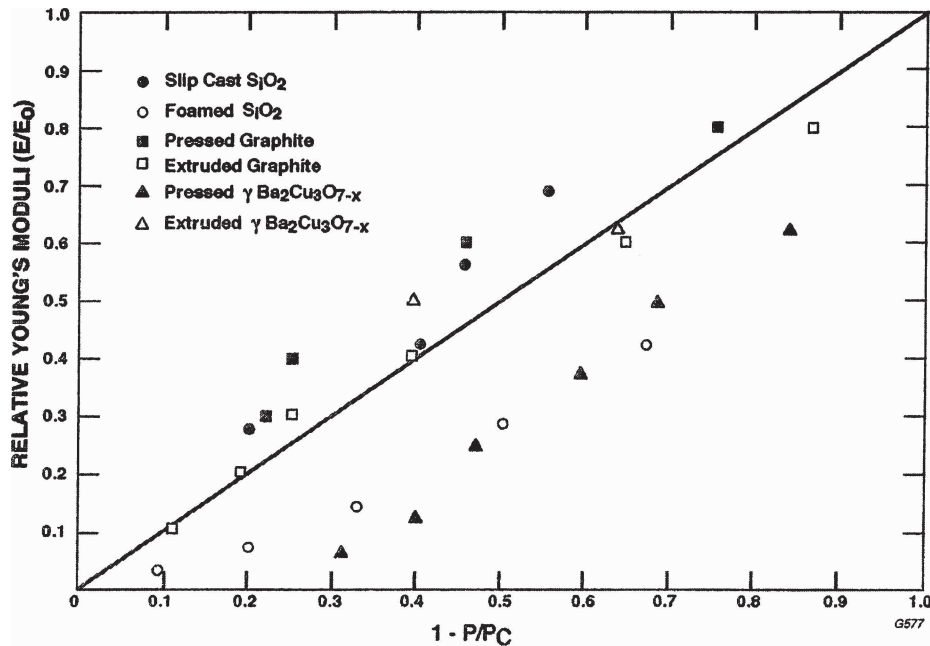


Figure 2 Linear plots for data and models of relative elastic moduli, i.e., of the elastic modulus at some porosity,  $P$ , to that at  $P = 0$  versus  $1 - P/P_C$ , i.e., where  $P$  normalized by  $P_C$ , the value of  $P$  where the elastic moduli must go to zero. (a) Plots of minimum solid area (MSA) models [2, 13, 14] for: (1) tubular pores aligned parallel ( $P_C \sim 1$ ) or (2) perpendicular ( $P_C \sim 0.8$ ) to the stress axis, (3) of simple cubic stacking of uniform spherical or (4) cubical pores ( $P_C \sim 1$ ). (b) Plots for MSA modes for simple cubic ( $\sim$  random) and denser (rhombohedral) packing of uniform spherical particles [2, 13, 14], for bodies of glass beads sintered to various degrees [15, 16], and for an alumina body pressed and sintered to various degrees [17]. Note all elastic moduli are Young's modulus, except for data of Berge *et al.* [16] is for bulk modulus. (c) Plots of slip cast silica sintered to various degrees [18], foamed silica [19], pressed [20] and extruded [21] graphite densified to various degrees, and a superconducting ceramic pressed [22, 23] and extruded [24]. The foamed and extruded bodies reflect higher  $P_C$  values and the slip cast or pressed bodies lower values. (Continued)





(c)

Figure 2 (Continued).

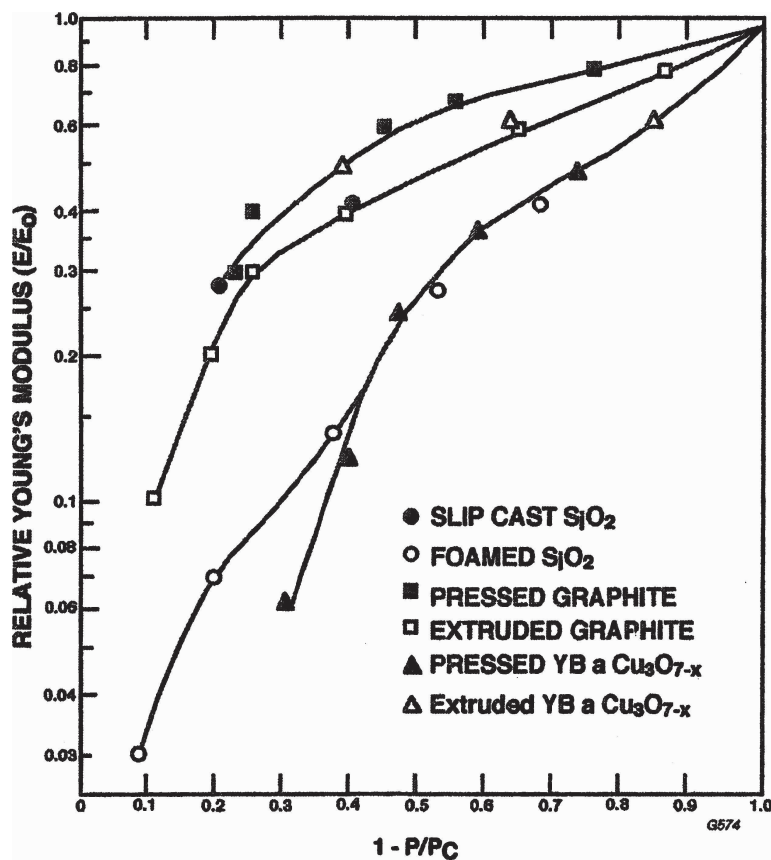


Figure 3 A semi log plot of the data of Fig. 2C versus  $1 - P/P_C$ . Note the nonlinear nature of the plots, their close spacing, and their overlapping, again illustrating the difficulties of distinguishing one curve from another. Note such plotting of the data sets from Fig. 2A and B results in even closer spacing and more overlap of the separate plots.

for tubular pores aligned normal to the stress axis, and still progressively more for pores between particles of various packings sintered to various degrees. Further, note that refinement of the  $P_C$  values is expected to further improve normalization consolidation and agreement. Such agreement strongly suggests some underlying common microstructural characteristic to the poros-

ity dependence of pertinent properties. It may also aid in differentiation of more successful models from less successful one in reflecting the porosity dependence on appropriate properties.

The success of  $P$  normalization of MSA models to essentially a single universal MSA plot versus limited consolidation for models of the form  $(1 - P)^n$  is

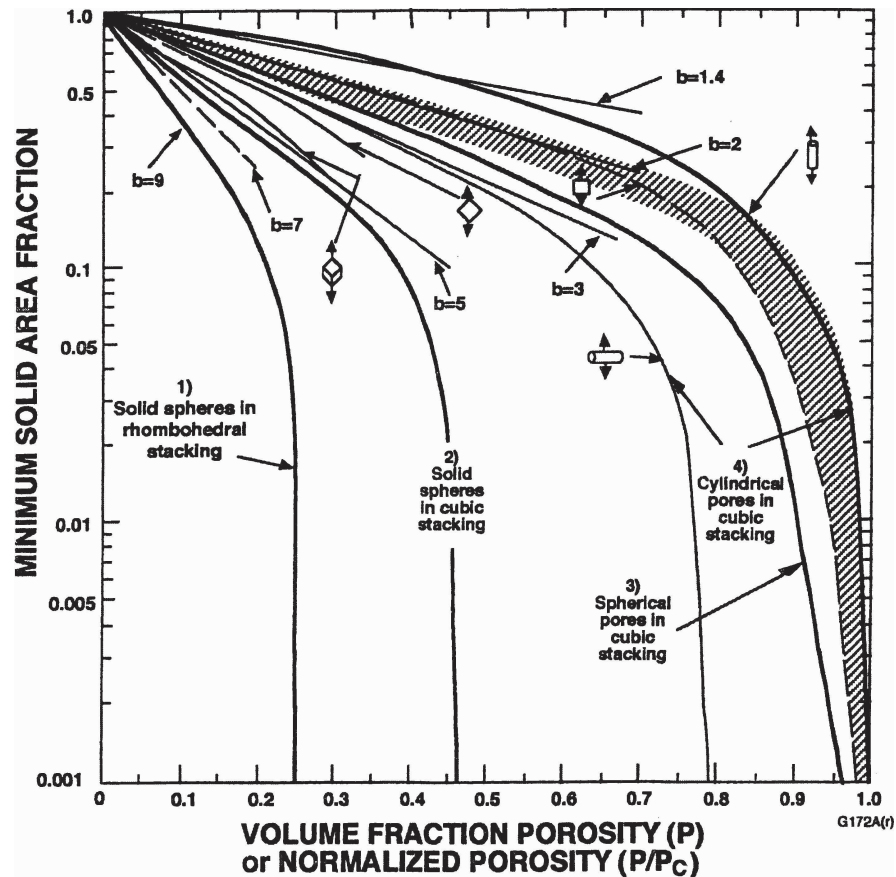


Figure 4 Semi log plot of key MSA models versus  $P$  and by  $P$  normalized by  $P_C$ , i.e., plotting MSA versus  $P/P_C$ . Such normalization brings the wide diversity of MSA models shown into a modest band (cross hatched area at or near the upperlimit of porosity dependent behavior, i.e., for tubular pores aligned with the stress axis). Note, approximate  $P_C$  values are readily obtained from the intersection of the curves with the porosity (horizontal) axis if they extend to low property values.

attributed to the latter reflecting little or no microstructural details while each MSA model for a given porosity reflects unique aspects of each pore-solid microstructure via two key parameters. These are first the nearly linear decrease of properties on a semilog plot versus  $P$  over about the first half of the applicable porosity range (i.e., the slopes,  $b$  values, of Fig. 4) and secondly the precipitous decrease of properties with increasing  $P$  at higher  $P$  where  $P \rightarrow P_C$ , with the latter being uniquely given by MSA models. Since both  $b$  and  $P_C$  are reflective of the specific pore-solid microstructure of each MSA model, it is not surprising that normalization of  $P$  with  $P_C$  results in normalizing the property-porosity behavior, i.e., since  $b$  and  $P_C$  are not independent, varying inversely with each other.

#### 4. Summary and conclusions

Normalization of porosity, i.e., use of  $P/P_C$  instead of  $P$  alone (where  $P_C$  is the value of  $P$  for which the porosity dependent properties go to zero), in a common power law model of the form  $(1 - P)^n$  clearly removes the limitation of this model that it does not go to zero property values for the many important cases where  $P_C < 1$ . However, while such normalization may compress the data some, it does not appear to distinguish differing behavior trends for differing types of porosity, a particular problem where models have no theoretical or empirical data base to at least indicate what differ-

ences in behavior are due to what type(s) of porosity are present in bodies of interest. Data fitting may be of limited aid in refining estimates of  $P_C$  values, but the primary determination of such values should be done mainly or exclusively by more direct means, mainly: (1) direct measurement as the porosity of green bodies of powder compacts with out binders, e.g., after binder burnout, (2) calculated from MSA idealized models, or (3) determined by extrapolation of semilog plots, as noted in Fig. 4. Whether porosity normalization of power law models of the form  $(1 - P)^n$  can lead to adequate identification of porosity types and  $n$  values or consolidation of curves for different porosity types into a universal plot is uncertain.

It was shown that normalization of  $P$  by  $P_C$  (which is a microstructurally sensitive factor) is applicable to other models; in particular consolidating MSA models into a single "universal" property-porosity curve. This normalization of MSA models is in marked contrast to the limited and variable effects that such normalization has on the leading power law model focused on mechanics with little or no microstructural input. While there are only two sets of cases evaluated here, the stark contrast in their normalization behavior indicates that the normalization behavior of MSA (and other possible microstructurally oriented models) adds to their credibility in representing the porosity dependence of mechanical properties. The consolidation to a single "universal" property-porosity curve also suggests that there is a

basic microstructural character to porous structures that underlies the diversity of porosity dependence for various porous structures. Thus, evaluation of the effects of  $P$  normalization on porosity-property models can be a useful tool in evaluating, developing, or using such models.

## References

1. C. W. BERT, *J. Mater. Sci.* **20** (1985) 2220.
2. R. W. RICE, "Porosity of Ceramics" (Marcel Dekker, New York, 1998).
3. K. K. PHANI, *J. Mater. Sci. Lett.* **5** (1986) 747.
4. K. K. PHANI and S. K. NIYOGI, *J. Mater. Sci.* **22** (1987) 257.
5. *Idem.*, *J. Amer. Cer. Soc.* C-362-66 (1987).
6. D. C. LAM, F. F. LANGE and A. G. EVANS, *ibid.* **77**(8) (1994) 2113.
7. T. OSTROWSKI, A. ZIEGLER, R. J. BORDIA and J. RÖDEL, *ibid.* **81**(7) (1998) 1852.
8. T. OSTROWSKI and J. RÖDEL, *ibid.* **82**(11) (1999) 3080.
9. A. P. ROBERTS and E. J. GARBOCZI, *ibid.* **83**(12) (2000) 3041.
10. A. R. DAY, K. A. SNYDER, E. J. GARBOCZI and M. F. THORPE, *J. Mech. Phys. Solids* **40**(5) (1992) 1031.
11. K. A. SNYDER, E. J. GARBOCZI and A. R. DAY, *J. Appl. Phys.* **72**(12) (1992) 5948.
12. J. KOVÁČIK, *J. Mater. Sci. Lett.* **20** (2001) 1953.
13. R. W. RICE, *J. Mater. Sci.* **31** (1996) 102.
14. *Idem.*, *ibid.* **31** (1996) 1509.
15. L. CORONEL, J. P. JERNOT and F. OSTERSTOCK, *ibid.* **25** (1990) 4866.
16. P. A. BERGE, B. P. BONNER and J. A. BERRYMAN, *Geophys.* **60**(1) (1995) 108.
17. D. J. GREEN, C. NADER and R. BREZNY, in "The Elastic Behavior of Partially-Sintered Alumina, Sintering of Advanced Ceramics," edited by C. A. Handwerker, J. E. Blendell and W. Kaysser (Am. Cer. Soc., Westerville, OH, 1990) p. 347.
18. G. M. TOMILOV, *Tr. from Izvestiya Akademii Nauk SSSR, Neorganicheskie Materialy* **13**(1) (1977) 117.
19. J. N. HARRIS and E. A. WELSH, "Fused Silica Design Manual, I," NSC Special Publication (1973) p. 5.
20. P. WAGNER, J. A. O'ROURKE and P. E. ARMSTRONG, *J. Amer. Cer. Soc.* **55**(4) (1972) 214.
21. E. A. BELSKAYA and A. S. TARABANOV, "Experimental Studies Concerning the Electrical Conductivity of High-Porosity Carbon-Graphitic Materials," Institute of High Temperatures, Academy of Sciences of the USSR, *Tr. from Inzhenerno-Fizicheskii Zhurnal* (1971) Vol. 20, No. 4, p. 654.
22. B. BRIDGE and R. ROUND, *J. Mat. Sci.* **8** (1989) 691.
23. J. P. SINGH, H. J. LEU, R. P. POEPEL, E. VAN VOORHEES, G. T. GOUDEY, K. WINSLEY and D. SHI, *J. Appl. Phys.* **66**(7) (1989) 3154.
24. N. MCALFORD, J. D. BIRCHALL, W. J. CLEGG, M. A. HARMER, K. KENDALL and D. H. JONES, *J. Mat. Sci.* **23** (1988) 761.

*Received 14 October 2004  
and accepted 20 September 2005*